Alterations in Mitochondrial Structure and Function Are Early Events of Dexamethasone-induced Thymocyte Apoptosis

Patrice X. Petit,* Hervé Lecoeur,‡ E. Zorn,‡ Charles Dauguet,‡ Bernard Mignotte,*§ and Marie-Lise Gougeon‡

*Centre de Génétique Moléculaire, CNRS, Bât. 24, 91198 Gif-sur-Yvette, France; ‡Unité d'Oncologie Virale, Département SIDA et Rétrovirus, Institut Pasteur, 75724 Paris Cedex 15, France; and §Université de Versailles Saint-Quentin, 78035 Versailles, France

Abstract. In this paper we used a multiparametric approach to analyze extensively the events occurring during apoptotic cell death of thymocytes, and furthermore, we asked whether alterations in mitochondrial structure and function are occurring in early stages of apoptosis. A multiparametric quantitative analysis was performed on normal or apoptotic thymocytes emerging from a few-hour culture performed in culture medium or in the presence of dexamethasone. Simultaneous detection of light scattering properties, integrity of plasma membrane (trypan blue exclusion), chromatin condensation (AO/EB staining of entire cells or PI staining of nuclei), and DNA fragmentation (in situ nick-translation in apoptotic cells) allowed a precise analysis of the preapoptotic and apoptotic stages. Moreover a thorough study of mitochondrial transmembrane potential ($\Delta\Psi_m$) assessed following in a time course study the uptake by apoptotic cells of the cationic lipophilic dye $DiOC_6(3)$ or the J-aggregate–forming cation JC-1, indicates that a drop in $\Delta\Psi_m$ occurs very early in thymocyte apoptosis, before DNA fragmentation. This is associated with alteration in mitochondrial structure assessed by cytofluorimetric study of NAO uptake in apoptotic cells. Finally these dramatic alterations in mitochondrial structure and function occurring in early stages of apoptosis were confirmed by confocal and electron microscopy analysis.

PROGRAMMED Cell Death (PCD)[1] of thymocytes is a crucial event that is involved in the negative intrathymic selection of the T cell repertoire, leading to the clonal deletion of autoreactive T cells and to the establishment of self-tolerance (10, 4). This death of physiological significance, called apoptosis, is an active process of self-destruction associated to profound structural changes including a nuclear collapse characterized by the condensation of chromatin and fragmentation of DNA into single and multiple oligonucleosomes leading to a final and irreversible cell destruction (2, 20, 46).

It was stated that no marked changes in energy metabolism were observed in apoptotic cells, and particularly the morphology and function of mitochondria were reported to be nonaffected in early apoptotic cells (9, 20, 21). However the finding that the anti-apoptotic activity of the *Bcl-2* proto-oncogene, which is located to the inner mitochondrial membrane (16), can be correlated to its ability to increase the mitochondrial membrane potential ($\Delta\Psi_m$) in L929 cells (15) suggests that mitochondrial function could be impaired during apoptosis. Moreover, a recent study we performed on rat embryo cells immortalized with temperature sensitive mutants of SV-40 large T antigen, showed that cells exhibiting the morphological features of apoptosis (at restrictive temperature, heat-inactivation of large T antigen causes p53 release, growth arrest, and cell death with apoptotic characteristics [48]) exhibited a decreased $\Delta\Psi_m$, correlated with an uncoupling of electron transport from ATP production. These events were detected at early stages of the apoptotic process when most of the cells were not irreversibly committed to death, suggesting that mitochondria could be a primary target during apoptosis of these cells (43).

To assess whether alterations of mitochondrial structure and function are occurring in apoptosis of immature thymocytes, we performed a multiparametric analysis of thy-

Address all correspondence to Dr. Marie-Lise Gougeon, Unite d'Oncologie Virale, Département SIDA et Rétrovirus, Institut Pasteur, 28 Rue du Dr. Roux, 75724 Paris cedex 15. Tel.: (33) 1 45 68 89 07. Fax: (33) 1 45 68 89 09.

1. *Abbreviations used in this paper*: AO, acridine orange; $\Delta\Psi_m$, mitochondrial membrane potential; $\Delta\Psi_{pm}$, plasma membrane potential; $DiOC_6(3)$, 3,3′-dihexyloxacarbocyanine iodide; EB, ethidium bromide; FSC, forward scatter; JC-1, 5,5′,6,6′-tetrachloro-1,1′,3,3′-tetraethylbenzimidazolcarbocyanine iodide; mClCCP, carbonylcyanide m-chlorophenylhydrazone; NAO, 10-N-nonyl acridine orange; PI, propidium iodide; SSC, side scatter.

mocytes undergoing apoptosis either spontaneously or after dexamethasone treatment. Simultaneous detection of light scattering properties, integrity of plasma membrane, chromatin condensation, and DNA fragmentation allowed a precise analysis of the preapoptotic and apoptotic stages. Futhermore, a thorough study of mitochondrial structure and function indicates that alterations in mitochondria are early events in thymocyte apoptosis, characterized by dramatic changes in mitochondrial membrane visualized by electron and confocal microscopy, associated with a drop of $\Delta\Psi_m$ occurring before oligonucleosomal DNA fragmentation.

Materials and Methods

Thymocytes Cultures

Thymocytes were isolated from male mice Balb/c (3–4 wk old) and cellular suspension was prepared according to Raffay and Cohen (36). Thymocytes were incubated for various periods of time, either at 4°C or at 37°C, at 1×10^6 cells/ml in RPMI-1640 supplemented with 10% (vol/vol) FCS, 1 mM glutamine, 10 mM Hepes, 1% penicillin/streptomycin. In some experiments 1 μM dexamethasone (9α-fluoro-16α-methyl-prednisolone; Sigma Immunochemicals, St. Louis, MO) was added at the initiation of the culture at 37°C.

Cellular Mortality

The cellular mortality was assessed according to the loss of trypan blue exclusion. Percentages of dead cells were estimated after counting 100 cells for each sample.

Gel Electrophoresis of Fragmented DNA

Gel electrophoresis of DNA was performed according to the method described by Newell et al. (29). 2×10^6 cells were lysed in 500 μl of 10 mM Tris, 1 mM EDTA, 0.2% Triton X-100. High and low molecular weight fractions from lysed cells were separated and the low molecular weight fractions, containing fragmented DNA, were precipitated at −20°C in 50% 2-propanol and 0.5 M NaCl. The precipitates were collected after centrifugation at 13,000 *g*, air-dried, resuspended in 10 mM Tris, 1 mM EDTA (pH 7.4), and treated with RNAse (Sigma) at 5 μg/ml during 30 mn at 36°C. Loading buffer containing 15 mM EDTA, 2% SDS, 50% glycerol, and 0.5% bromophenol blue was added to samples at 1:5 (vol/vol), and samples were heated to 65°C for 10 min. Electrophoresis was performed in 0.75% agarose for 2 h, 90V. Oligonucleosomal fragments of DNA were visualized by staining with ethidium bromide.

Quantitation of Apoptosis by Flow Cytometric Analysis

Nick-Translation Assays. As one of the major characteristics of apoptosis is DNA-fragmentation, we quantitated cells exhibiting DNA breaks using the in situ nick-translation technique originally described by Meyaard et al. (26) that we slightly modified. After successive fixations of the cells in 1% paraformaldehyde for 20 min at 0°C and in 70% ethanol for 4 min, DNA breaks were nick-translated for 90 min in 10 μl of a mixture containing 55 μM of dUTP-biotine (Boehringer Mannheim Corp., Indianapolis, IN), 19 μM of dATP, dCTP, dGTP (Pharmacia Biotech Inc., Piscataway, NH), 100 U/ml of DNA-polymerase I (Promega, Madison, WI), in 50 mM Tris-HCL, 5 mM $MgCl_2$, 10 mM β-mercaptoethanol, 10 μg/ml BSA, pH 7.8. The cells were washed in PBS, and the labeling was realized for 30 min in 40 μl of a mixture containing 20 μg/ml of RNAse DNAse-free (Boehringer Mannheim Corp.), 5 μg/ml of avidin-FITC (InterbioTech, Paris, France), 0.1% Triton X-100, 5% (wt/vol) nonfat milk powder, in 4× SSC. Flow cytometry analysis was performed on a FACScan (Becton Dickinson, San Jose, CA) tuned at 488 nm, using the FL1 photomultiplier (bandpass 530 nm, bandwidth 30 nm). The data were recorded in list mode for further analysis with the lysis II software (Becton Dickinson).

Acridine Orange (AO)/Ethidium Bromide (EB) Staining. We described previously this double staining which allows to distinguish early apoptotic cells from living and dead cells (12, 33). 2.5×10^5 pelleted thymocytes were resuspended in 200 μl of PBS. 2 μl of staining solution (stock solution AO 1.5 μg/ml, EB 5 μg/ml) were added and the cell suspension was incubated for 5 mn at room temperature.The cell suspension was then diluted with 200 μl of PBS and analyzed with a FACScan. EB is used to stain dead cells, emitting a red-orange fluorescence with a 488-nm laser excitation. Using the same excitation, AO emits a yellow-green fluorescence when bound to a DNA and a red-orange fluorescence with RNA. However with the very low AO concentration used, only DNA emits enough fluorescence intensity to be detected under these conditions. The photomultipliers were FL1 for AO and FL2 (bandpass 585 nm, bandwidth of 42 nm) for EB. Using this assay, we observed not only the dead and viable cell populations usually described in fluorescent staining, but also a third population. The latter was weakly stained with AO and unstained with EB, and analysis of the forward light scatter signal (FSC) (cell size) of cells in this population showed that they exhibit a reduced size (see Fig. 1). The correlation between the subdiploid DNA content, as suggested by the weaker AO staining, and the existence of DNA fragments characteristic of apoptosis in these cells was previously shown in experiments separating them from dead cells and living cells on percoll gradients. Gel electrophoresis of DNA from these separated populations showed a characteristic DNA scale associated with cells weakly stained with AO or dead cells, whereas this was not observed in DNA from living cells (33).

Nuclei Staining with Propidium Iodide (PI). Quantification of apoptotic nuclei was assessed by staining apoptotic nuclei with PI and performing FACS analysis according to a method previously described by Nicoletti et al. (30). Briefly pelleted cells were gently resuspended in 1.5 ml of hypotonic fluorochrome solution (PI 50 μg/ml in 0.1% sodium citrate, 0.1% Triton X-100). After overnight incubation, PI fluorescence was determined by FACScan analysis. Apoptotic nuclei appeared as a broad hypodiploid DNA peak that was easily distinguished from the narrow peak of nuclei with normal (diploid) DNA content in the red fluorescence channel (see Fig. 1).

Cytofluorimetric Analysis of $\Delta\Psi_m$ and Mitochondrial Structure

$\Delta\Psi_m$ Assessment Using $DiOC_6(3)$ and JC-1 Dyes. Variations of the mitochondrial transmembrane potential $\Delta\Psi_m$ during thymocyte apoptosis were studied using 3,3′-dihexyloxacarbocyanine iodide ($DiOC_6(3)$; Molecular Probes, Inc., Eugene, OR). This cyanine dye accumulates in the mitochondrial matrix under the influence of the $\Delta\Psi_m$ (6). $2.5\ 10^5$ thymocytes were incubated in 100 μl of PBS containing 0.1 μM of $DiOC_6(3)$ for 30 min. $DiOC_6(3)$ membrane potential-related fluorescence was recorded using FL1 PMT.

$\Delta\Psi_m$ variations were also analyzed with another cyanine, 5,5′,6,6′-tetrachloro-1,1′,3,3′-tetraethylbenzimidazolcarbocyanine iodide (JC-1; Molecular Probes) (37, 41). 2.5×10^5 thymocytes were incubated in 100 μl of PBS containing 0.1 μM of JC-1 for 30 min. For the FACScan acquisition, the PMT values were 524V and 429V, respectively, for FL1 and FL2; the FL1-FL2 compensation was 3% and FL2-FL1 compensation was 21%.

Mitochondrial Structure Analysis Using NAO. Alteration of mitochondrial structure during thymocyte apoptosis has been evaluated following Nonyl Acridine Orange (10-*N*-nonyl -3,6-bis[dimethylamino]acridine) or NAO incorporation (34, 35). 2.5×10^5 thymocytes were incubated in 100 μl of PBS containing 4 μM of NAO for 30 min. Samples were followed for FACScan analysis with the same photomultiplier setting than used for $DiOC_6(3)$. The red fluorescence was recorded on the FL2 PMT for a control but not routinely used (34, 35).

αβ F1-ATPase Status of Cultured Thymocytes

The amount of αβ F1-ATPase was compared in living thymocytes incubated during 16 h at 4°C, and apoptotic thymocytes following 16-h culture at 37°C in the absence or in the presence of 1 μM dexamethasone, as described above. Cells were then rinsed twice in cold PBS, collected in isolation buffer containing sucrose 0.32 M, TES 5 mM pH 7.4, EDTA 0.5 mM, and lysed by addition of 0.5% Nonidet P-40. Crude extracts (50–100 μg of protein) were used for Western blotting. Proteins were transferred to nitrocellulose. Blots were exposed overnight at 4°C to the rabbit anti-αβF1–ATPase polyclonal antibody (kindly provided by P. Vignais, Centre d'Etude Nucléaire, Grenoble, France) and then exposed 1 h at room temperature to horseradish peroxidase-conjugated anti-immunoglobulin serum (Biosis, Philadelphia, PA). The immunoreactivity was revealed using Amersham ECL kit as described by Zheng et al. (48).

Confocal Microscopy

Thymocytes were examined with a MRC-600 confocal microscope (Bio-Rad Labs., Richmond, CA) equipped with a 25 mW argon-ion laser and two detector channels. Excitation was performed using the 488-nm line from the argon-ion laser. Using an appropriate combination of filters, fluorescence emission was divided into yellow/green (515–540 nm) and red (570 nm and above) components that were directed through different confocal apertures to the two separate photomultipliers. The red fluorescence of the propidium iodide was used to discard the dead cells from the picture taken with the yellow/green channel. Confocal sections were made at increments of 0.3 μm. Maximum brightness projections (25) of parts of the complete 3-D data set of optical sections were performed. The dye concentrations were 0.1 μM for $DiOC_6(3)$ and NAO, 0.05 μM for JC-1 and 2.5 μg/ml for PI.

Electron Microscopy

Ultrastructural morphology of mitochondria and nuclei in entire cells was performed by electron microscopy. Cells were fixed in 2.5% glutaraldehyde, 4% osmic acid, and 1% tannic acid. They were then dehydrated in a series of alcohol solutions and embedded in Epon. Sections were stained with uranyl acetate and lead citrate before examination with a JEM 1200 EXII electron microscope.

Results

Multiparametric Flow Cytometry Analysis of Apoptotic Thymocytes

One of the problems associated with cell death study is the lack of common and reliable marker of apoptosis. Indeed, internucleosomal DNA-fragmentation is often considered as a hallmark of apoptosis. As shown on Fig. 1, panel *5*, nucleosomal ladder can easily be detected after electrophoresis of DNA from thymocytes cultured during 24 h at 37°C in the absence of stimulation (Fig. 1, *5* lane *B*) while it is not observed when thymocytes are maintained at 4°C (Fig. 1, *5* lane *A*). A significant increase of apoptosis can be induced in thymocytes by glucocorticoids (7) and as shown in Fig. 1, *5* lane *C*, the intensity of the nucleosomal bands is enhanced when thymocytes are incubated with dexamethasone. Internucleosomal DNA-fragmentation is a common feature of apoptosis, as it occurs in most cases. However it is not observed in all cases of apoptosis and therefore cannot be relied on exclusively as a marker of apoptosis (8, 32).

Morphological modifications of cells undergoing apoptosis, which can be precisely analyzed by flow-cytometry, represent one of the criteria used to quantify apoptosis. Thymocytes undergoing apoptosis exhibit a smaller size (FSC) and a higher granulosity (SSC) as compared to living cells (2, 9, 21). As shown in Fig. 1, *1 A*, thymocytes incubated overnight at 4°C are not altered in their viability whereas their culture at 37°C allows to distinguish three distinct populations (Fig. 1, *1 B*): apoptotic cells (*green*) exhibit size and granulosity criteria easily distinguishable from living cells (*blue*) and dead cells (*red*). When dexamethasone is added at the initiation of 24-h culture of thymocytes (Fig. 1, *1 C*), most of the cells are undergoing apoptosis, and FSC/SSC analysis reveals that thymocytes fall either in the early apoptotic population or in the dead cell population. Although following the size criteria is convenient, it is also restrictive since cells committed to this cell death undergo continuous modifications that cannot be analyzed with this parameter alone. Therefore, to follow accurately the alterations occurring during the apoptosis process, we performed a multiparametric approach allowing to correlate on the same apoptotic population the cellular and nuclear modifications.

Morphological and nuclear modifications occurring during apoptosis were assessed following several methods. The first one allows to distinguish apoptotic, but still living, cells from dead cells by dual staining with AO and EB. Living thymocytes (Fig. 1, *2 A*) are highly stained by AO and do not incorporate EB. When thymocytes are incubated overnight at 37°C, one can distinguish several populations (Fig. 1, *2 B* and *C*): apoptotic cells, which exhibit a reduced size (*green*) are weakly stained with AO as compared to living cells and unstained by EB because of a limited permeabilization of their plasma membrane, whereas dead cells (*red*) are even smaller and stained with EB. Therefore comparison between *1* and *2* in Fig. 1 indicates that one of the stages of apoptosis is characterized by cell volume alteration but preservation of plasma membrane permeabilization. This early apoptotic population (*green*) can be distinguished from the late apoptotic one (*red*) which has totally lost cell integrity. Quantification of apoptosis on the basis of nuclear modifications, such as chromatin condensation, can also be performed by staining apoptotic nuclei with PI (30). FACScan analysis of stained nuclei from cultured thymocytes shows the existence of two peaks, a narrow fluorescent peak with normal DNA content and a broad hypodiploid DNA peak, corresponding to apoptotic nuclei (Fig. 1, *4 B*). The percentage of apoptotic nuclei (52%) correlates with the proportion of apoptotic cells detected by AO/EB staining. However we must point out that PI staining of nuclei seems to underestimate the proportion of apoptotic cells in the population of dexamethasone-treated thymocytes (Fig. 1, *4 C*). Therefore, in that case, discrimination between apoptotic cells with condensed chromatin and normal cells is more accurate using AO staining. Identification of apoptotic cells can also be performed by in situ nick-translation (26) which allows the quantification of cells with fragmented DNA (Fig. 1, *3*). A good correlation was found when assessment of apoptotic cells by nick translation was compared to FSC/SSC analysis or AO/EB staining (Fig. 1, *1–3*): as deduced previously from size analysis, the majority (98%) of dexamethasone-treated thymocytes and 57% of 37°C-incubated thymocytes are apoptotic and 3′end-labeling indicates that they exhibit fragmented DNA. It is worth noting that multiparametric analysis of thymocytes has revealed a heterogeneity in apoptotic populations, distinguishing an early apoptotic population with reduced size, nuclear alterations including DNA fragmentation but preservation of plasma membrane permeabilization, from a late apoptotic population with different light scattering properties and loss of membrane integrity.

Analysis by Flow Cytometry of Mitochondrial Modifications Occurring during Apoptosis

$\Delta\Psi_m$ Evaluation with a Cyanine Dye, $DiOC_6(3)$. During apoptosis, the plasma membrane of thymocytes undergoes multiple changes. These include morphological alterations as revealed by electron microscopy (27, 46), reduction of lectin binding sites, reduced expression of several thymocyte an-

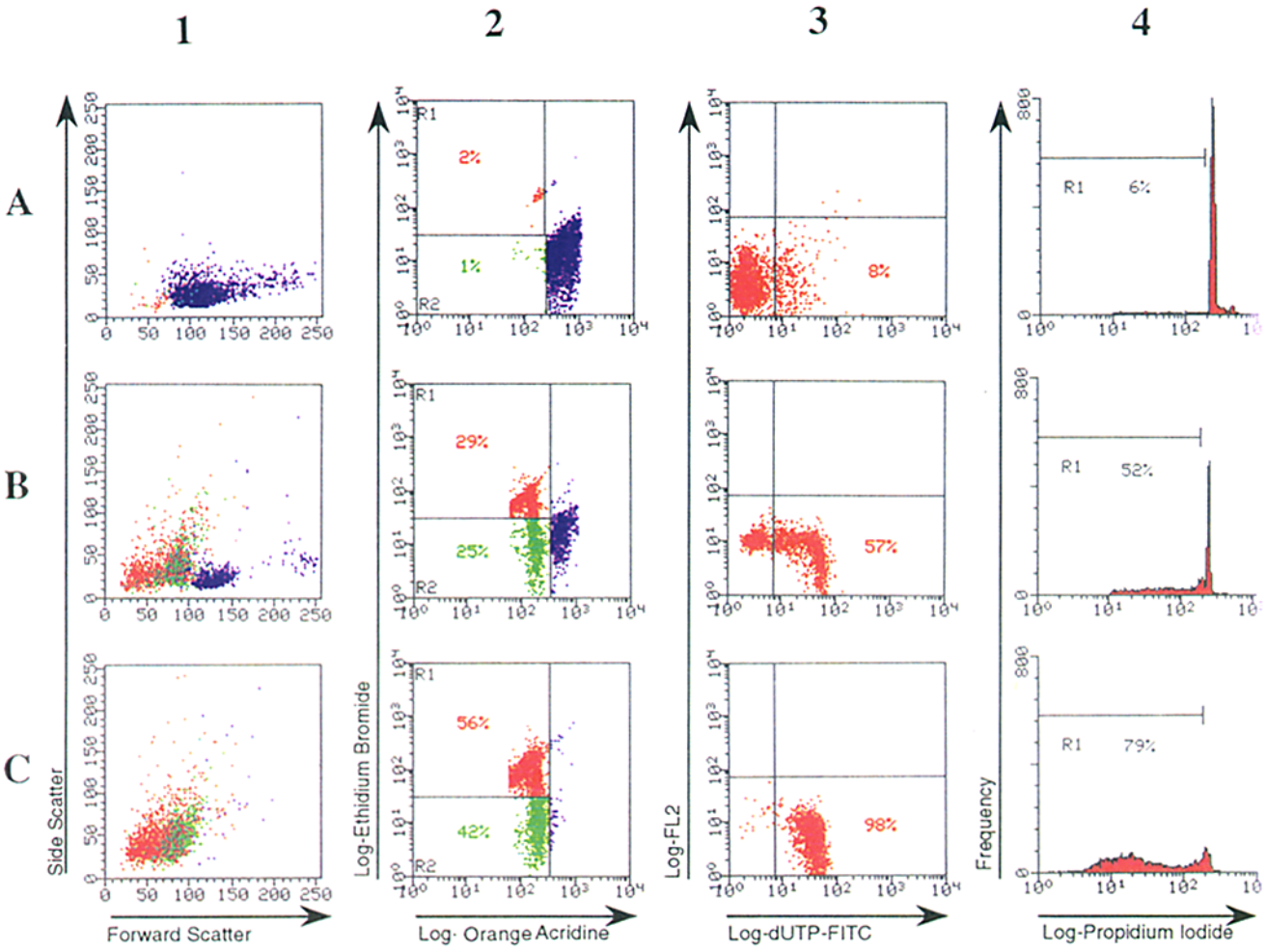

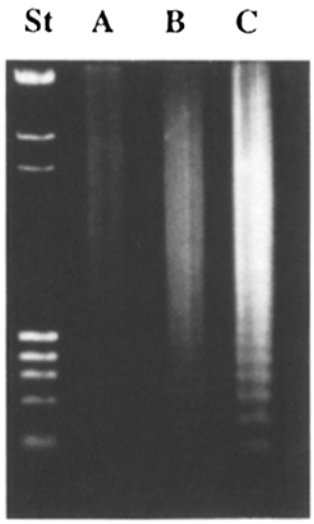

5

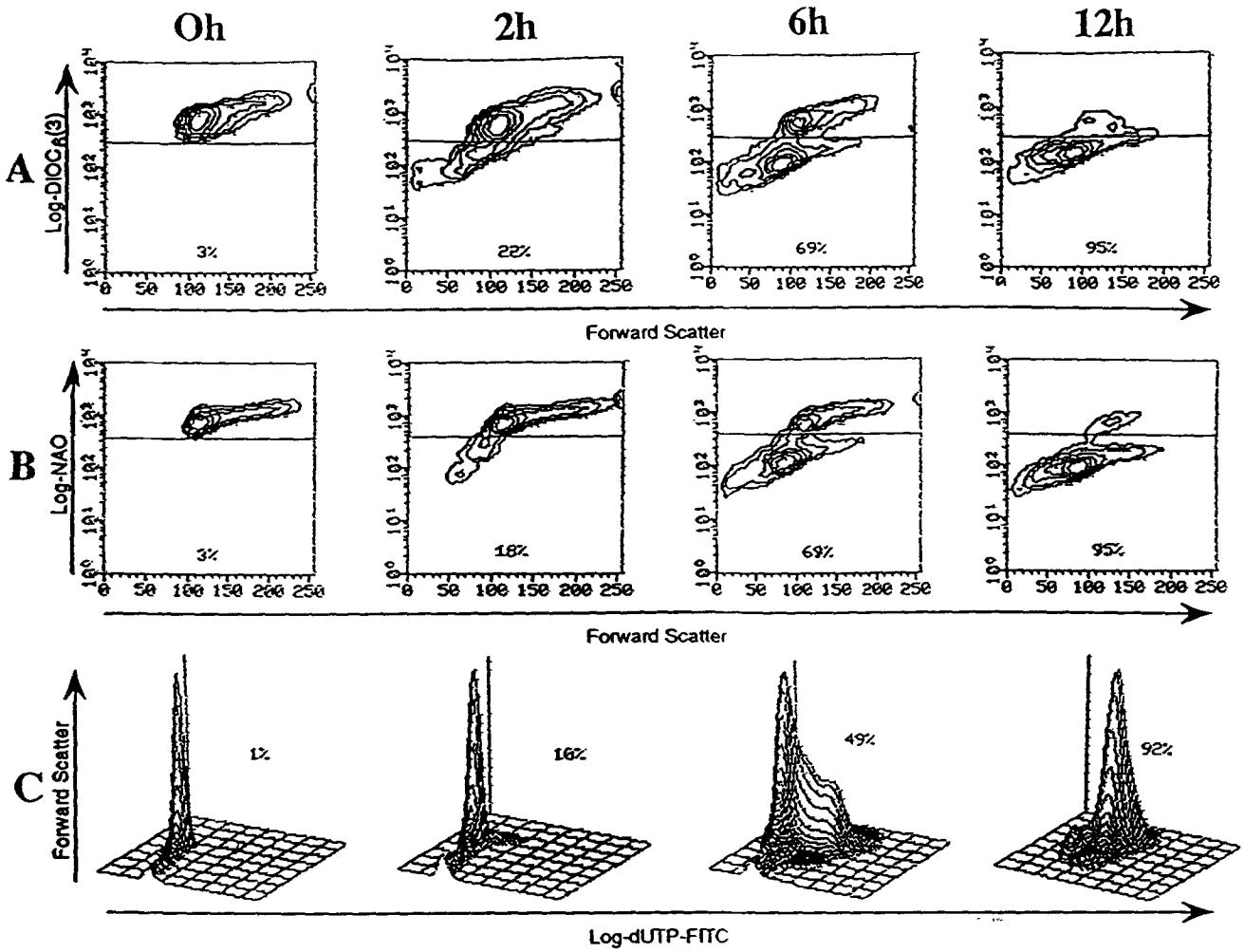

Figure 2. Mitochondrial modifications occuring in dexamethasone-treated thymocytes. Cytofluorimetric time course analysis of mitochondrial alterations in thymocytes incubated during 16 h with 1 μM dexamethasone. (*A*) Mitochondrial membrane potential-related fluorescence of $DiOC_6(3)$. (*B*) Mitochondrial membrane structure changes recorded by NAO fixation onto cardiolipin. (*C*) Quantification of DNA fragmentation by nick-translation assay.

tigens (8) including CD4 and CD8 (42) and changes in membrane lipids (11). We analyzed with several specific dyes the mitochondrial modifications occuring during apoptosis of dexamethasone-treated thymocytes. Following fluorescence associated with the uptake of cationic lipophilic dye $DiOC_6(3)$ allows to evaluate $\Delta\Psi_m$ modifications. Fig. 2 *A* shows a time-course study of membrane potential-related fluorescence of $DiOC_6(3)$ after staining of dexamethasone treated thymocytes. It can be observed that cells undergoing morphological changes over time, which can be detected by the FSC parameter, show simultaneously a marked decrease of $\Delta\Psi_m$-related fluorescence. This drop in mitochondrial potential is observed 2 h after dexamethasone treatment and concerns at that time 22% of thymocytes, and it increases with time until 12 h after dexamethasone treatment where the majority (95%) of thymocytes show a drop in mitochondrial potential. Therefore $\Delta\Psi_m$ modifications, evaluated by the uptake of cationic lipophilic dye $DiOC_6(3)$, are detected early in the process of apoptosis.

Mitochondrial Membrane Modifications Assessed with NAO Staining. Alteration of mitochondrial structure has been evaluated following NAO incorporation in the same dexamethasone-treated thymocyte population mentioned above. Considering that a cardiolipid molecule binds two molecules of NAO, any decrease in fluorescence will mean either a decreased amount of cardiolipids into the mitochondrial membrane or a drastic alteration of them (35).

Figure 1. Multiparametric quantitative flow cytometric analysis of thymocytes undergoing apoptosis. Thymocytes were incubated during 16 h either at 4°C (*A*) or at 37°C in culture medium (*B*) or in the presence of 1 μM dexamethasone (*C*). Several parameters were followed on these populations. (*1*) Analysis of morphological modifications assessed by light scattering properties i.e., FSC and SSC; (*2*) Analysis of cell death by dual staining with acridine orange and ethidium bromide; (*3*) detection of cells with fragmented DNA by in situ nick translation; (*4*) detection of apoptotic nuclei by propidium iodide staining; and (*5*) gel electrophoresis of DNA from thymocyte populations. Lane *St*, DNA markers; (lane *A*) thymocytes incubated at 4°C; (lane *B*) thymocytes incubated at 37°C; (lane *C*) thymocytes treated with 1 μM dexamethasone.

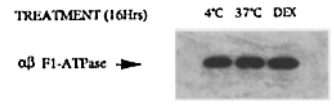

Figure 3. Comparison of αβF1-ATPase status of living vs. apoptotic thymocytes. Thymocytes were incubated during 16 h either at 4 or at 37°C in culture medium or in the presence of 1 μM dexamethasone. The amount of αβF1-ATPase was determined as described in Materials and Methods.

Fig. 2 *B* shows that reduction of FSC observed 2 h after dexamethasone treatment is accompanied by a drop in NAO-related fluorescence. Interestingly, comparison of $DiOC_6(3)$ and NAO fluorescence in the same time course study of apoptotic thymocytes (Fig. 2, *A* and *B*) indicates that the same percentages of cells show a reduction in $\Delta\Psi_m$ and an alteration of mitochondrial membrane structure. A careful parallel study of fluorescence associated with these two dyes did not allow one to determine which event precedes the other during the first 2 h of culture (data not shown). The drop in $\Delta\Psi_m$ impairs mitochondrial protein import and may impair the cardiolipin synthesis. As a consequence, it may modify the ratio of respiratory chain component to cardiolipin, subsequently reducing the cardiolipin staining with NAO.

A simultaneous determination of thymocytes undergoing DNA breaks by in situ nick-translation (staining with dUTP) (Fig. 2 *C*) indicates that cells with fragmented DNA can be found 2 h after dexamethasone treatment. It is noteworthy that the percentages of cells stained by dUTP two and 6 h after dexamethasone treatment are significantly lower than the proportion of cells showing impairment in $\Delta\Psi_m$ and mitochondrial membrane (Fig. 2, compare *C* with *A* and *B*). It suggests that during apoptosis mitochondrial alterations may occur before DNA fragmentation. However DNA degradation is known to occur in two steps. The first one, which results in fragments of 300 and 50 kb, precedes internucleosomal degradation (5). Since the first step may not be detected by the nick-translation procedure, we cannot exclude that DNA degradation to large fragments may occur at the same time, or even before the observed changes in mitochondria.

In order to exclude the possibility that the observed decrease in uptake of $DiOC_6(3)$ and decreased stainability with NAO was a consequence of shedding of apoptotic bodies (which include mitochondria), the αβF1-ATPase status of thymocytes maintained either at 4°C for 16 h, or induced to apoptosis at 37°C or by treatment with dexamethasone was analyzed by Western blotting and immunoreactivity (Fig. 3). Whatever the culture conditions used, i.e., whether thymocytes were alive or apoptotic, no difference in the amount of these essential components of the inner mitochondrial membrane was found. Together with our electron- and confocal microscopy observations (see below), these results argue that the changes we observed at the mitochondrial level during the process of apoptosis do not originate from a decreased number of mitochondria per cell but rather are the consequences of alterations in mitochondrial structure and function.

Electron Microscopy Analysis. Electron microscopy anal-

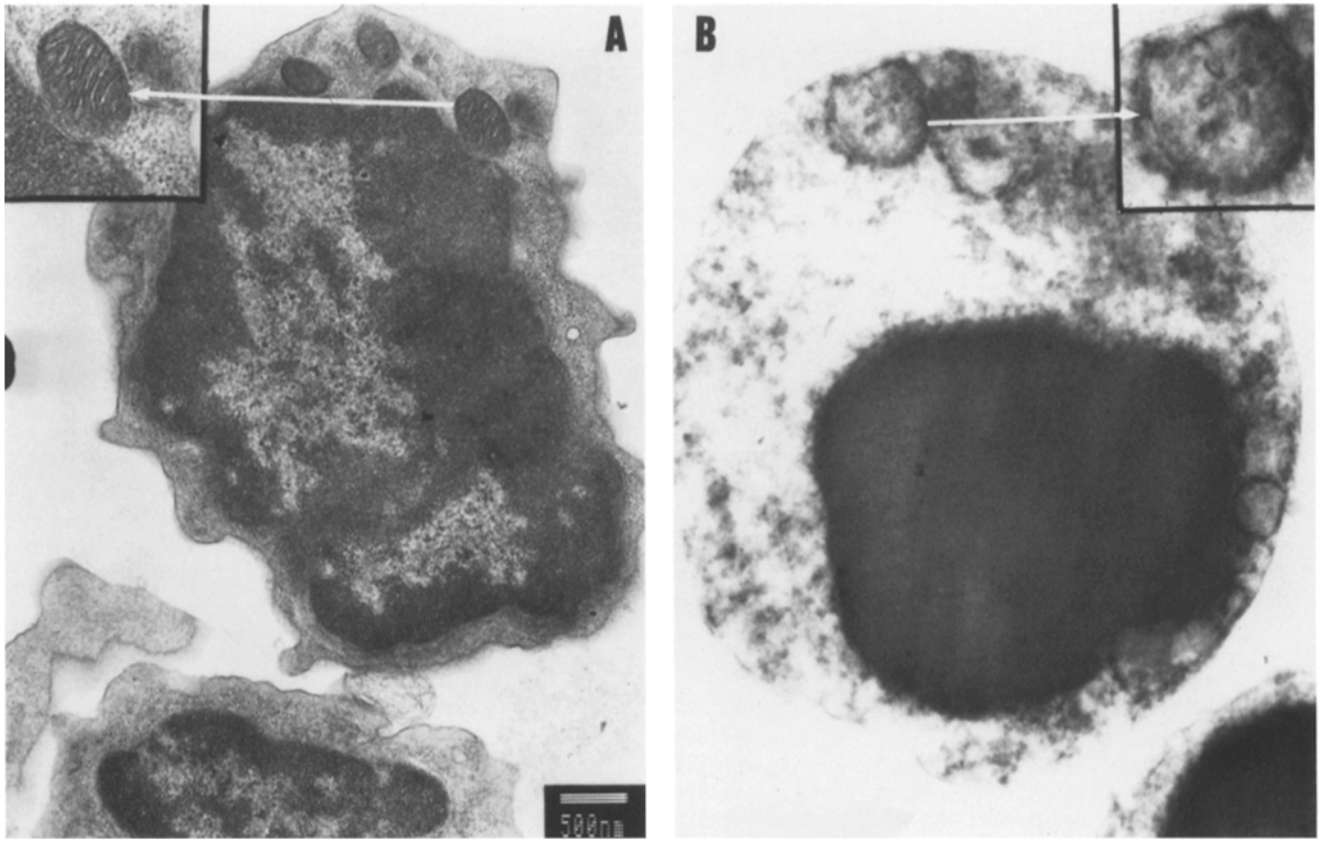

Figure 4. Electron microscopy analysis of mitochondrial alterations. (*A*) Normal thymocytes and (*B*) dexamethasone-treated apoptotic thymocytes showing condensed chromatin associated to profound alteration of mitochondria ultrastructure.

ysis visualized mitochondrial alterations suggested by the flow-cytometric analysis. Fig. 4 compares mitochondria from either living thymocytes incubated overnight at 4°C or dexamethasone-treated apoptotic thymocytes. In living thymocytes the chromatin is normal and mitochondrial structures are preserved (Fig. 4 *A*). Apoptotic thymocytes harbor simultaneously the nuclear characteristic of apoptotic cells (i.e., condensation of nuclear chromatin), and dramatic alterations of the mitochondrial structures (i.e., reduction of the number of cristae membranes, destructurization of the surrounding membranes, and swelling of the organelles) (Fig. 4 *B*).

Time Course Analysis of Early Events during Apoptosis

Fig. 5 is a detailed kinetic of mitochondrial and nuclear modifications detectable during the first twelve hours of dexamethasone-induced apoptosis. Since a previous time course study of mitochondrial alterations indicated that $DiOC_6(3)$ and NAO related fluorescence followed the same kinetic (Fig. 3), we only show in Fig. 5 results obtained with $DiOC_6(3)$. A drop in $\Delta\Psi_m$ is observed very early and after 1 h 10% of thymocytes show mitochondrial dysfunction when fragmentation of DNA or staining with trypan blue are not yet detected. After 4 h of incubation the gap between cells exhibiting a drop in $\Delta\Psi_m$ and cells with fragmented DNA is important: when 40% of thymocytes show a decrease in $DiOC_6(3)$-related fluorescence, only 20% of cells undergo DNA-fragmentation. At that time, apoptotic cells are not able to incorporate trypan blue. It is striking to note that plasma-membrane permeabilization, evaluated by trypan blue staining, is a very late phenomenon occuring after mitochondrial and nuclear alterations. In that sense the time 6 h is very characteristic: only 10% of thymocytes are considered as apoptotic if one refers to trypan blue staining whereas $\Delta\Psi_m$ evaluation indicates that 70% of them are committed to apoptosis. After 12 h the whole population of thymocytes share the monitored features of apoptosis.

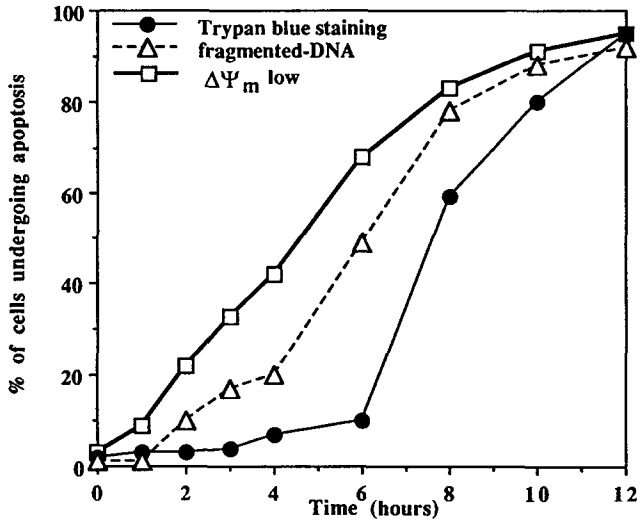

Figure 5. Time-course analysis of early events in dexamethasone-induced apoptosis. Quantification of cells undergoing apoptosis was performed following three parameters: (*a*) percentage of cells exhibiting a low $\Delta\Psi_m$-related fluorescence assessed by $DiOC_6(3)$ staining; (*b*) percentage of cells with fragmented DNA assessed by in situ nick translation; and (*c*) percentage of cells incorporating the trypan blue.

Therefore this time course multiparametric study has revealed the existence of a very early apoptotic stage in which thymocytes show mitochondrial alterations such as a drop in $\Delta\Psi_m$ whereas intact membrane permeability is preserved and internucleosomal DNA degradation is not detected. Mitochondrial alterations appear therefore to be an early event observed as a part of the apoptotic process in thymocytes.

Flow Cytometry and Confocal Microscopy Analysis of the $\Delta\Psi_m$ with the J-Aggregate-forming Cation, JC-1

Lipophilic cations such as cyanines dyes and rhodamine 123 have been used to probe mitochondrial membrane potential in living cells (6). However it is not clear that all mitochondria within one cell necessarily adopt identical membrane potentials. JC-1 has the unique property of forming J-aggregates locally and spontaneously under high mitochondrial $\Delta\Psi_m$ (which fluoresces in red) whereas the monomeric form fluoresces in green (37, 41). Such dyes may be useful reporter molecules for localized biochemical events if one can overcome the problems posed by the small amount of thymocyte cytoplasm.

The staining of thymocytes with JC-1 at 0.25 μM allows one to measure an internal heterogeneity in the mitochondrial $\Delta\Psi_m$ within the cells. A clear difference appears between the green-fluorescence of the monomers and the red fluorescence of the J-aggregates that depends on magnitude of the $\Delta\Psi_m$. Living thymocytes exhibit at the same time intensive green and red fluorescences (Fig. 6, *2 A*). Apoptotic thymocytes, identified by their light scattering properties (reduced FSC and increased SSC) (Fig. 6, *1 B* and *C, blue*) exhibit an extinction of the red fluorescence (Fig. 6, *2 B* and *C*) similar, to a certain extent, to what could be obtained by the incubation of thymocytes with an uncoupler like mClCCP (2.5 μM) (data not shown). Therefore using the JC-1 dye, these observations extend the results described above on the membrane potential-related fluorescence of $DiOC_6(3)$ and confirm that mitochondrial $\Delta\Psi_m$ alteration occurs during apoptosis.

Due to the small amount of thymocyte cytoplasm, it is difficult to follow by confocal microscopy the spatial changes occurring between JC-1–related green and red-fluorescence during induction of apoptosis. Fig. 7, *B* shows that nonapoptotic cells exhibit a wide JC-1 fluorescence heterogeneity at the mitochondrial level since mitochondria appear simultaneously red and green. When apoptosis is induced by dexamethasone, the decrease in $\Delta\Psi_m$ (indicated by the flow-cytometric analysis, Fig. 6) induces the extinction of the red fluorescence and only a residual green fluorescence is visible at the mitochondrial level (monomeric form of JC-1) (data not shown). Within the cytoplasm a green fluorescence of JC-1 is also visible, which may be due to the maintenance of the plasma membrane potential. Only a treatment of the cells with an uncoupler like mCICCP would totally abolish this green JC-1 fluorescence (37, 41).

Confocal microscopy analysis visualized the mitochon-

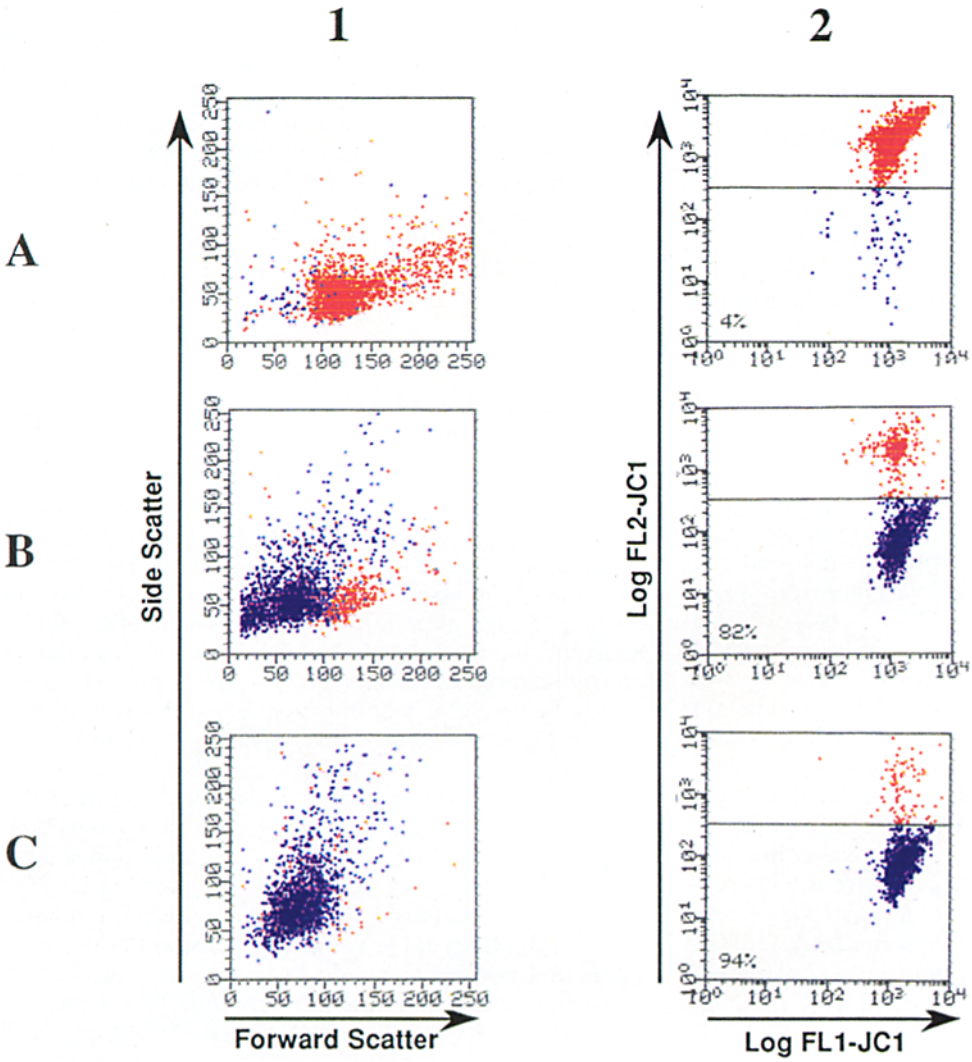

Figure 6. Flow cytometric analysis of thymocytes stained with the J-aggregate forming lipophilic cation JC-1. Thymocytes were incubated during 16 h either at 4°C (*A*) or at 37°C in culture medium (*B*) or in the presence of 1 μM dexamethasone (*C*). Biparametric cytograms show the FSC/SSC parameters (panel 1) or FL1(*green*)/FL2(*red*) (*2*) fluorescence of JC-1–stained cells. Control with mClCCP as a decoupling agent has been performed as a test of the $\Delta\Psi_m$-related red fluorescence of the dye (data not shown).

drial modifications occurring in an apoptotic cell and correlated them to nuclear modifications. Fig. 7, *C* and *D* shows dual staining of living (*C*) or apoptotic thymocytes with NAO and PI. While a living cell exhibits an absence of PI-staining of nuclei associated to a marked NAO-related fluorescence, an apoptotic cell shows a complete extinction of NAO fluorescence conjugated to an important PI fluorescence in nuclei. These pictures confirm the results we obtained with the cytofluorimetric approach indicating that mitochondrial alterations combined to chromatin condensation are important features of thymocyte apoptosis.

Discussion

The present report shows that alterations in mitochondrial structure and function are early events of thymocyte apoptosis. Until recently, it was generally assumed that mitochondria were morphologically normal during apoptotic cell death, whereas in necrotic cells they appeared swollen. However, some data indicate that a breakdown of mitochondrial function could be occuring during apoptosis. An inhibition of oxidative ATP production has been reported to be associated with glucocorticoid-induced lymphocyte apoptosis (31) and a decreased mitochondrial dehydrogenase ability to cleave tetrazolium salt (MTT) (28) has been found in anti-CD3–induced apoptosis of T cell hybridoma (44). In the case of TNF_α-induced apoptosis (24), early disruption of mitochondrial function (23, 39) has been described. Recently we have shown that, during the commitment to apoptosis of cell conditionally immortalized with SV-40, there is an early drop of $\Delta\Psi_m$ (which correlates with an uncoupling of electron transport from ATP production), a drop in the rate of mitochondrial protein translation and a drop in the maturation of mitochondrial protein cytoplasmic precursors (43). In the present paper we show that in the model system of thymocyte apoptosis, a similar drop in $\Delta\Psi_m$ is also an early event. Thus, this $\Delta\Psi_m$ alteration is an early marker of apoptosis in at least two cell systems, and possibly more generally. Our results are in close connection with a recent study showing that an early drop of $\Delta\Psi_m$ is observed in response to different agents inducing lymphoid cell depletion in vivo (47), and interestingly this reduction in $\Delta\Psi_m$ was shown to be an irreversible step of ongoing lymphocyte death, preceding other alterations of cellular physiology such as DNA degradation into high and low molecular weight fragments (47).

Is this breakdown of mitochondria directly involved in

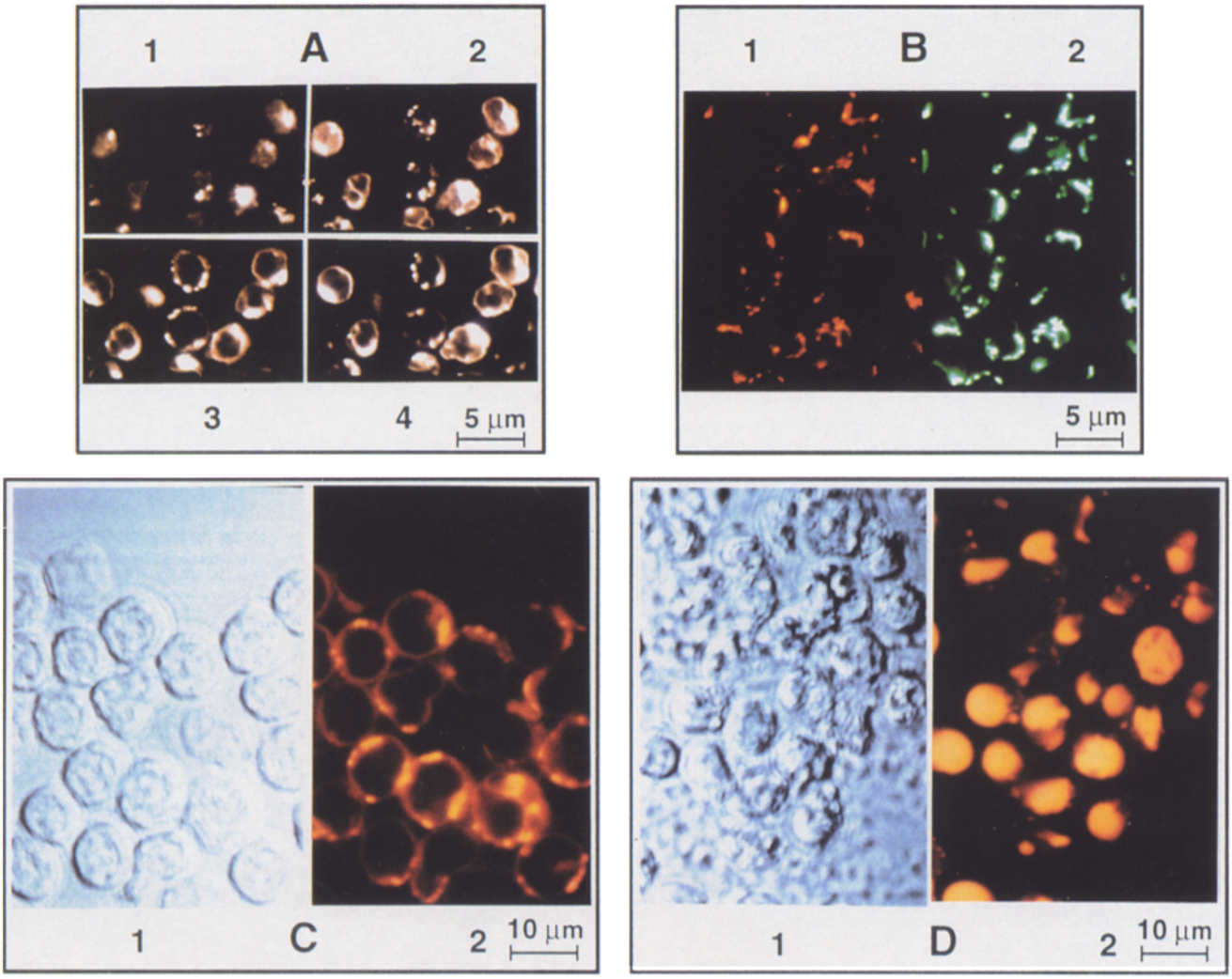

Figure 7. Confocal microscopy analysis of apoptotic thymocytes stained with $DiOC_6(3)$, JC-1 and NAO/PI. (*A*) $DiOC_6(3)$ staining of normal thymocytes. 1–4 represent four confocal sections of the same thymocyte preparation with 0.3 μm distance between each section. (*B*) JC-1 staining of normal thymocytes. (*1*) Red fluorescence of the J-aggregates and (*2*) Green fluorescence of the monomeric form of the dye. (*C*) Normal thymocytes (16 h at 4°C). (*1*) Phase contrast picture and (*2*) PI/NAO staining: mitochondrial NAO staining associated to unstained nuclei. (*D*) Apoptotic thymocytes (1 μM dexamethasone, 16 h at 37°C). (*1*) Phase contrast picture showing characteristic "blebbs" and (*2*) PI/NAO staining: extinction of mitochondrial NAO fluorescence associated to PI staining of apoptotic nuclei.

the apoptosis process? The finding that the *Bcl2* protooncogene product can locate to mitochondrial membrane (16) and that its ability to suppress apoptosis is reduced in constructs that lack the COOH-terminal transmembrane segment (1, 17) has suggested that mitochondrial function could be actively impaired during apoptosis and that *Bcl2* could counteract this event. The observation that *Bcl2* can block apoptosis in cells that do not contain a functional respiratory chain (cells lacking mtDNA) (18) has brought the conclusion that apoptosis itself and the anti-apoptotic activity of *Bcl2* are not related to mitochondrial respiration. However several arguments are in favor of the involvement of a mitochondrial event in apoptosis. (*a*) The cells devoid of mtDNA had been selected for their ability to grow in the presence of ethidium bromide which inhibits mtDNA replication. During the selection most cells die (by apoptosis?) and therefore the clones are selected for their ability to grow and survive in the absence of respiration. Furthermore, these cells generate ATP by glycolysis and also maintain a normal $\Delta\Psi_m$ probably by using the ADP/ATP translocator to import ATP in the mitochondria (40). (*b*) L929 cells overexpressing *bcl-2* have an increased $\Delta\Psi_m$ and are protected against apoptotic cell killing induced by TNFα. TNFα-mediated cytotoxicity in L929 cells has also been shown to alter mitochondrial structure and to inhibit succinate- and NADH-dehydrogenase activity. This inhibition of the electron transport becomes readily detectable 1 h after TNFα addition, thus preceding the onset of cell death by at least 3–6 h. (*c*) Specific mitochondrial respiratory chain inhibitors like rotenone and antimycin A and the highly specific ATP-synthase inhibitor oligomycin induce an apoptotic response in mammalian cells including L929 fibroblasts (45), indicating that a drop in $\Delta\Psi_m$ is sufficient to induce the other events of an apoptotic cell death. (*d*) The *Caenorhabditus elegans* and *Caenorhabditus briggsae* Ced9 genes, functional homo-

logues of *bcl-2*, have been cloned (14). In both nematode species they are expressed as a polycistronic mRNA with the cytB560 mRNA. Thus, evolution has selected and conserved a coexpression of these two genes suggesting a possible functional link. Furthermore this cytochrome belongs to the complex II which is entirely built of nuclearly encoded proteins and thus can exist in cells devoided of mtDNA.

The origin of the mitochondrial alterations remains undetermined. Taking into account that *Bcl2* functions in an antioxidant pathway to prevent apoptosis (17, 19) we can propose two alternative explanations. Since it has been described that prooxidants induce calcium release from mitochondria (38) and that $\Delta\Psi_m$ is dependent on mitochondrial calcium uptake (13), we can suppose a model where free radicals induce a release of mitochondrial calcium which itself mediates the drop of $\Delta\Psi_m$. A repartitioning of intracellular calcium has indeed been observed during apoptosis in several cases (3, 22). However *bcl-2* does not seem to affect Ca^{2+} uptake by mitochondria (22). Alternatively we can imagine that the breakdown of mitochondria observed during apoptosis leads to an increased production of free radicals and that *bcl-2* (or *ced-9)* can counteract their effect. This implies that an increase in free radical production would be observed during apoptosis, even in cells devoid of mtDNA. However, to our knowledge, such a production of prooxidants in a cell that does not contain a full respiratory apparatus has not been reported.

The authors would like to acknowledge M.-G. Enouf and C. Axler (Institut Pasteur) for their excellent technical assistance, Dr. J. L. Vayssiere (Centre de Génétique Moléculaire [C. G. M.]) for helpful discussions and Dr. R. Karess (C. G. M) for the critical reading of the manuscript.

This work was supported by grants from the Agence Nationale de Recherche sur le SIDA, the Association pour la Recherche sur le Cancer (6960 to B. Mignotte), the Ligue Nationale Contre le Cancer, the Centre National de la Recherche Scientifique, the European Community Biomed-1 program (BMH1-CT92-1571) and the Pasteur Institute.

Received for publication 19 August 1994 and in revised form 11 April 1995.

References

1. Alnemri, E. S., N. M. Robertson, T. F. Fernandes, C. M. Croce, and G. Litwack. 1992. Overexpressed full-length human Bcl-2 extends the survival of baculovirus-infected sf9 insect cells. *Proc. Natl. Acad. Sci. USA.* 89: 7295–7299.
2. Arends, M. J., and A. H. Wyllie. 1991. Apoptosis: mechanisms and roles in pathology. *Int. Rev. Exp. Pathol.* 32:223–254.
3. Baffy, G., T. Miyashita, J. R. Williamson, and J. C. Reed. 1993. Apoptosis induced by withdrawal of interleukin-3 (IL-3) from an IL-3-dependent hematopoietic cell line is associated with repartitioning of intracellular calcium and is blocked by enforced bcl-2 oncoprotein production. *J. Biol. Chem.* 268:6511–6519.
4. Blackman, M., J. A. Kappler, and P. Marrack. 1990. The role of the T-cell receptor in positive and negative selection of developing T cells. *Sciences* 248:1335–1340.
5. Brown, D. G., X. M. Sun, and G. M. Cohen. 1993. Dexamethasone-induced apoptosis involves cleavage of DNA to large fragments prior to internucleosomal fragmentation. *J. Biol. Chem.* 268:3037–3039.
6. Chen, L. B. 1988. Mitochondrial membrane potential in living cells. *Annu. Rev. Cell Biol.* 4:155–181.
7. Cohen, J. J., and R. C. Duke. 1984. Glucocorticoid activation of a calcium-dependent endonuclease in thymocyte nuclei leads to cell death. *J. Immunol.* 132:38–42.
8. Cohen, G. M., X. M. Sun, R. T. Snowden, D. Dinsdale, and D. N. Skilleter. 1992. Key morphological features of apoptosis may occur in the absence of internucleosomal DNA fragmentation. *Biochem. J.* 286:331–334.
9. Darzynkiewicz, Z., S. Bruno, G. Delbino, W. Gorczyca, M. A. Hotz, P. Lassota, and F. Traganos. 1992. Features of apoptotic cell measured by flow cytometry. *Cytometry.* 13:795–808.
10. Ellis, R. E., J. Y. Yuan, and H. R. Horvitz. 1991. Mechanisms and functions of cell death. *Annu. Rev. Cell Biol.* 7:663–698.
11. Fadok, V. A., D. R. Voelker, P. A. Cambell, J. J. Cohen, D. L. Bratton, and M. Henson. 1992. Exposure of phosphatidylserine on the surface of apoptotic lymphocytes triggers specific recognition and removal by macrophages. *J. Immunol.* 18:2207–2216.
12. Gougeon, M. L., S. Garcia, D. Guétard, R. Olivier, C. Dauguet, and L. Montagnier. 1992. Apoptosis as a mechanism of cell death in peripheral lymphocytes from HIV1-infected individuals in Immunology of HIV infection (G. Janossy, B. Autran, F. Miedema, editors) A. G. Karger, Basel. 115–126.
13. Gunter, T. E., and D. R. Pfeiffer. 1990. Mechanisms by which mitochondria transport calcium. *Am. J. Physiol.* 258:C755–786.
14. Hengartner, M. O., and H. R. Horvitz. 1994. *C. elegans* cell survival gene Ced-9 encodes a functional homologue of the mammalian proto-oncogene Bcl-2. *Cell.* 76:665–676.
15. Hennet, Y., C. Richter, and E. Peterhans. 1993. Tumour necrosis factor-α induces superoxide anion production in mitochondria of L929 cells. *Biochem. J.* 289:587–592.
16. Hockenbery, D., G. Nunez, C. Milliman, R. D. Schreiber, and S. J. Korsmeyer. 1990. Bcl-2 is an inner mitochondrial protein that blocks programmed cell death. *Nature (Lond.).* 348:334–336.
17. Hockenbery, D. M., Z. N. Oltvai, X. M. Yin, C. L. Milliman, and S. J. Korsmeyer. 1993. Bcl-2 functions as an anti-oxidant pathway to prevent apoptosis. *Cell.* 75:241–251.
18. Jacobson, M. D., J. F. Burne, M. P. King, T. Miyashita, J. C. Reed, and M. C. Raff. 1993. Bcl-2 blocks apoptosis in cells lacking mitochondrial DNA. *Nature (Lond.).* 361:365–369.
19. Kane, D. J., T. A. Sarafian, R. Anton, H. Hahn, E. B. Gralla, J. S. Valentine, T. Ord, and D. E. Bredesen. 1993. Bcl-2 inhibition of neural death-decreased generation of reactive oxigen species. *Science (Wash. DC).* 262:1274–1277.
20. Kerr, J. F. R. 1971. Shrinkage necrosis: a distinct mode of cellular death. *J. Pathol.* 105:13–20.
21. Kerr, J. F. R., and B. V. Harmon. 1991. Apoptosis: the molecular basis of cell death. *Curr. Commun. Cell & Mol.* Biol. 3:5–29.
22. Lam, M., G. Dubyak, L. Chen, G. Nunez, R. L. Miesfeld, and C. Distelhorst. 1994. Evidence that Bcl-2 represses apoptosis by regulating endoplasmic reticulum-associated Ca^{2+} fluxes. *Proc. Natl. Acad. Sci. USA.* 91: 6569–6573.
23. Lancaster, J. R., S. M. Laster, and L. R. Gooding. 1989. Inhibition of target cell mitochondrial electron transfer by tumor necrosis factor. *FEBS (Fed. Eur. Biochem. Soc.) Lett.* 248:169–174.
24. Laster, S. M., J. G. Wood, and L. Gooding. 1988. Tumor necrosis factor induces both apoptotic and necrotic forms of apoptosis. *J. Immunol.* 141: 2629–2634.
25. Laurent, M., G. Johannin, H. Le Guyader, and A. Fleury. 1992. Confocal scanning optical microscopy and three dimensional imaging. *Biol. Cell.* 76:113–124.
26. Meyaard, L. S. A. Otto, R. R. Jonker, M. J. Mijnster, R. Keet, and F. Miedema. 1992. Programmed death of T cells in HIV-1 infection. *Science (Wash. DC).* 257:217–219.
27. Morris, R. G., A. D. Hargreaves, E. Duvall, and A. H. Wyllie. 1984. Hormone-induced cell death. Surface changes in thymocytes undergoing apoptosis. *Am. J. Pathol.* 115:426–436.
28. Mosman, T. 1983. Rapid colorimetric assay for cellular growth and survival: application to proliferation and cytotoxic assays. *J. Immunol. Methods.* 65:55–63.
29. Newell, M. K., L. J. Haughn, C. R. Maroun, and M. Julius. 1990. Death of mature T cells by separate ligation of CD4 and the T cell receptor for antigen. *Nature (Lond.).* 347:286–288.
30 Nicoletti, I., G. Migliorati, M. C. Pagliacci, F. Grignani, and C. Riccardi. 1991. A rapid and simple method for measuring thymocyte apoptosis by propidium iodide staining and flow cytometry. *J Immunol. Methods.* 139: 271–279.
31. Nordeen, S. K., and D. A. Young. 1976. Glucocorticoid action on rat thymic lymphocytes. *J. Biol Chem.* 251:7295–7303.
32. Oberhammer, F. A., M. Pavelka, S. Sharma, R. Tiefenbacher, A. F. Purchio, W. Bursch, and R. Schulte-Hermann. 1992. Induction of apoptosis in cultured hepatocytes and in regressing liver by transforming growth factor β1. *Proc. Natl. Acad. Sci. USA.* 89:5408–5412.
33. Olivier, R., O. Lopez, M. Mollereau, T. Dragic, D. Guetard, L. Montagnier. 1994. Prevention of early cell death in peripheral blood lymphocytes of HIV-infected individuals by an anti-oxidant: N-Acetyl Cysteine. In Oxidatif stress, cell activation and viral infection. C. Pasquier, editor. Birkauser. Verlag, Basel. 323–332.
34. Petit, P. X., J. O'Connor, D. Grunwald, and S. C. Brown. 1990. Analysis of the membrane potential of rat- and mouse-liver mitochondria by flow cytometry and possible applications. *Eur. J. Biochem.* 194:389–397.
35. Petit, J. M., O. Huet, P. F. Gallet, A. Maftah, M. H. Ratinaud, and R. Julien. 1994. Direct analysis and significance of cardiolipid transverse distribution in mitochondrial inner membranes. *Eur. J. Biochem.* 220:871–879.
36. Raffay, M., and G. M. Cohen. 1991. Bis(tri-n-butylin)oxide induces programmed cell death (apoptosis) in immature thymocytes. *Arch. Toxicol.*

65:135–139.
37. Reers, M., T. W. Smith, and L. B. Chen. 1991. J-aggregate formation of a carbocyanine as a quantitative fluorescent indicator of membrane potential. *Biochemistry.* 30:4480–4486.
38. Richter, C., and G. E. N. Kass. 1991. Oxidative stress in mitochondria: its relationship to cellular Ca^{2+} homeostasis, cell death, proliferation and differentiation. *Chem. Biol. Interactions.* 77:1–23.
39. Schulze-Osthoff, K., A. C. Bakker, B. Vanhaesebroeck, R. Beyaert, W. A. Jacob, and W. Fiers. 1992. Cytotoxic activity of tumor necrosis factor is mediated by early damage of mitochondrial functions. *J. Biol. Chem.* 267: 5317–5323.
40. Skowronek, P., O. Haferkamp, and G. Rodel. 1992. A fluorescence-microscopic and flowcytometric study of HeLa cells with an experimentally-induced respiratory deficiency. *Biochem. Biophys. Res. Commun.* 187:991–998.
41. Smiley, S. T., M. Reers, C. Mottolahartshorn. M. Lin, A. Chen, T. W. Smith, G. D. Steele, and L. B. Chen. 1991. Intracellular heterogeneity in mitochondrial membrane potentials revealed by a J-aggregate forming lipophilic cation JC-1. *Proc. Natl. Acad. Sci. USA.* 88:3671–3675.
42. Swat, W., L. Ignatowicz, and P. Kisielow. 1991. Detection of apoptosis of immature thymocytes by flow cytometry. *J. Immunol Methods.*137:79–87.
43. Vayssière, J. L., P.X. Petit, Y. Risler, and B. Mignotte. 1994. Commitment to apoptosis is associated with changes in mitochondrial biogenesis and activity in SV40 conditional cell lines. *Proc. Natl. Acad. Sci. USA.* 91: 11752–11756.
44. Vukmanovic, S., and R. Zamoyska. 1991. Anti-CD3-induced cell death in T cell hybridomas. Mitochondrial failure and DNA fragmentation are distinct events. *Eur. J. Immunol.* 21: 419–424.
45. Wolvetang, E. J., K. L. Johnson, K. Krauer, S. J. Ralph, and A. W. Linnane. 1994. Mitochondrial respiratory chain inhibitors induce apoptosis. *FEBS (Fed. Eur. Biochem. Soc.)Lett.* 339:40–44.
46. Wyllie, A. H., J. K. R. Kerr, and A. R. Currie. 1980. Cell death: the significance of apoptosis. *Int. Rev. Cytol.* 68:251–305.
47. Zamzami, N., P. Marchetti, M. Castedo, C. Zanin, J.-L. Vayssiere, P. X. Petit, and G. Kroemer. 1995. Reduction in mitochondrial potential constitutes an early irreversible step of programmed lymphocyte death in vivo. *J. Exp. Med.* 181:1661–1672.
48. Zheng, D. Q., J. L. Vayssière, H. Lecoeur, P. X. Petit, A. Spatz, B. Mignotte, and J. Feunteun. 1994. Apoptosis is antagonized by large T antigens in the pathway to immortalization by polyomaviruses. *Oncogene.* 9: 3345–3351.